Design of a Permanent Magnet Synchronous Motor for Submersible Installations as Part of a Photovoltaic Pump System

St. Henneberger, S. Van Haute, K. Hameyer and R. Belmans

Katholieke Universiteit Leuven
E.E. Dept., Div. ESAT/ELEN
Kardinaal Mercierlaan 94, B-3001 Leuven - Heverlee, Belgium

Abstract
As there is a demand for more powerful photovoltaic irrigation systems than offered now, the application of permanent magnet synchronous motors (PMSM) is a logical step, due to the higher efficiency they have compared to induction motors, especially at partial load. Therefore a 3.8 kW PMSM for submersible installations is designed and developed for "open loop" operation by implementing an additional rotor cage in order to avoid a position sensor. The design process combines analytical calculations with the finite element method (FEM). Minimising losses and other design aspects a submersible installation has to fulfill, such as the high reliability, are discussed. The need that the motor has to be perfectly adapted to the pump, as well as to the inverter in order to obtain a high efficiency of the overall system is considered .

1. INTRODUCTION

Most of the existing photovoltaic irrigation systems offer a mechanical output power from 0.85 kW up to 2.2 kW. Surface applications for irrigation systems are driven by dc machines while for installations in the drilling holes induction machines are used. However, small induction motors have, when compared with permanent magnet motors, a lower efficiency, whereas dc machines are not applicable for submersible installations.

The installed output power of the solar cells, being the most expensive part of the system, may be decreased by using permanent magnet motors and is profitable if it is taken into consideration that in future terms the demand for the installed power is expected between 3.5 kW and 5 kW.

Photovoltaic systems have to reach a high efficiency during approximately seven hours a day, in which more than 80% of the total daily solar energy is available (figure 1). This corresponds to the requirement that the motor operates with low losses in a large power range, from 50% to 100% of its rated power.

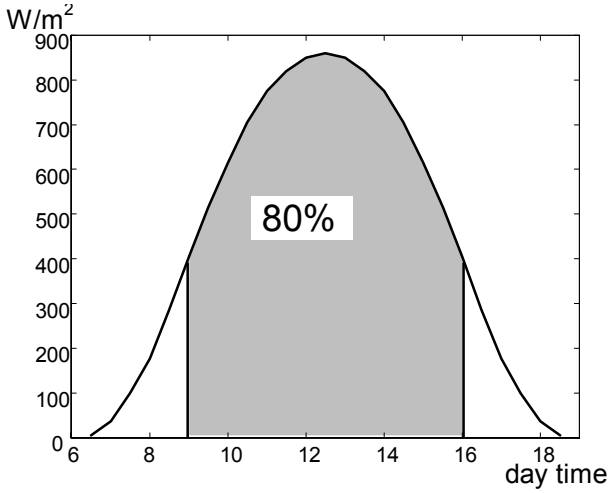

Fig. 1: Available solar energy in the Sahel area

2. THE PHOTOVOLTAIC PUMP SYSTEM

The design specifications are derived from the requirements of the application. The parameters of the other components of the drive form the constraints for the development of the motor, due to the fact that the efficiency of the overall system has to be considered.

By studying the drive concept (figure 2) it is obvious that the motor is the only component where a relatively high improvement of the efficiency can be realized, especially at partial load where PMSMs are far more efficient than induction machines.

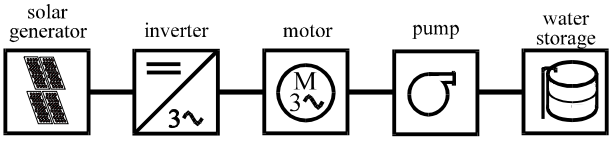

Fig. 2: Photovoltaic pump system

2.1 Solar generator

The installed output power of the solar panels is estimated to be 6 kW peak. Taking the irradiation data of an average day in the Sahel-area into account, the installed solar power corresponds to a total available energy of 22 kWh/day. If 18 modules (15 V, 50 W peak) are connected in series, the solar generator has an output voltage of 270 V. In contrast to most of the existing systems, operating at 80 V up to 120 V, the higher voltage is chosen in order to limit the current, reducing the motor size, the cost of the semi-conductor components of the inverter, the inverter losses and the conduction losses between the solar generator and the inverter.

2.2 Inverter

A short study of the solar inverter market learns that almost no inverter fulfills all requirements of the system under development., because most commercially available inverters for solar generators are suited for induction motors. Furthermore, the optimisation of the overall system requires output frequencies up to 70 - 80 Hz. However, the development and assembly of a new inverter would increase substantially the cost of the overall photovoltaic pumping system. As a compromise, a standard V/f controlled inverter is modified and adapted, adding maximum power point (MPP) tracking and specific protection measures, ensuring reliable operation under severe conditions.

The core of the inverter are IGBT power modules with 20 A rated current. The efficiency of the inverter is expected to be above 95 %. The use of a modified standard inverter offers the advantage that a certain degree of flexibility in voltage of the installed solar cells can be retained.

2.3 Pump

According to the envisaged installed power range, a centrifugal pump is chosen. According to the constraints set by the PMSM, the pump has the highest efficiency in the range of 1500 to 2200 RPM and a maximum mechanical power of 4 kW (figure 3). The optimum working conditions of this pump are found at a total manometric head between 12 and 18 m. However, this can be adapted by adjusting the impeller.

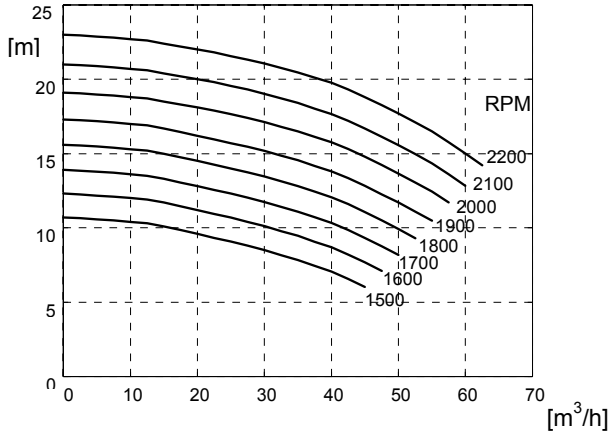

Fig. 3a: Flow rate as a function of the manometric head for different speeds

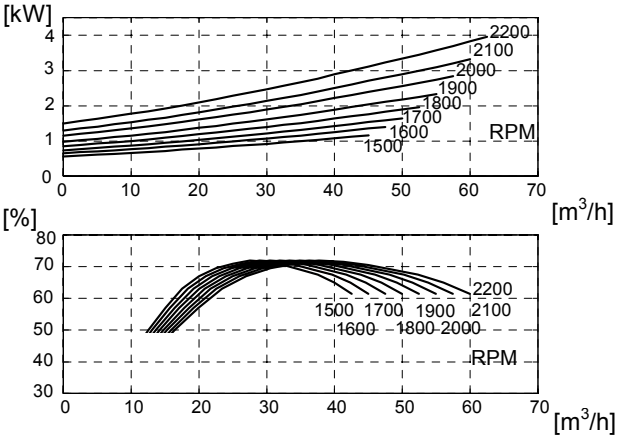

Fig. 3b: Required power and efficiency as a function of the flow rate

3. THE MOTOR DESIGN

3.1 Design methods

In a first step the motor is designed by analytical calculations being based on generalized electric machine theory [1], [2]. A PMSM can be modelled by

mathematical equations subject to the following assumptions:

- Ferromagnetic materials have an infinite permeability.
- Tooth and slot effects can be adequately accounted for by Carter's Coefficient [3].

Thus, the analytical calculation contains a lot of empirical formulations which have to be checked by numerical field analysis. When a motor model is found, the necessary data are created to start a finite element calculation. The FEM is an accurate method for electromagnetic field calculations, since it takes into account the nonlinearity of all magnetic materials, the detailed rotor and stator structure and the distribution of the stator windings. More than one finite element solution is required in order to find the parameters that have to be checked. In order to evaluate the steady state torque, as found from the analytical solution, only one solution is required. If the torque ripple is to be assessed, the solution must be repeated for multiple rotor positions. The magnets have to be checked against demagnetization. This can be done by supplying the transient short circuit current to the model and by evaluating the demagnetization in the model. From two solutions, the d- and q-axis inductances are found.

3.2 Reducing the losses

The highest efficiency for this 4-pole PMSM is required and has to be provided by reducing the losses, taking into account that the weight and the costs of the motor are of minor importance when compared to the costs of the solar cells. The losses in the stator iron increase with the flux density and the frequency:

$$P_{iron} \sim \left(\frac{B_{iron}}{1.5\,T}\right)^2 \cdot \left(\frac{f}{50\,Hz}\right)^2 \qquad (1)$$

The frequency is fixed so the iron losses are decreased by reducing the flux density by using more iron in the stator. Iron losses are further reduced by choosing thin low-losses iron laminations in the stack of the stator. The conduction losses

$$P_{iron} = I^2 \cdot R \qquad (2)$$

are reduced by using larger cross sections for the copper, that means larger stator slots. The motor frame however, is fixed to a certain limit, as the typical diameter of a drill-hole for drinkable water is 15 cm.

The wide flux paths and the large stator slots on the one hand and the limited motor diameter on the other hand reduce the rotor diameter and thus the torque. This has to be compensated by an increased length of the motor.

Half closed slots reduce the slot harmonics which are responsible for iron losses and eddy current losses in the permanent magnets. However, due to the relatively large effective air gap caused by the magnets, the openings of the stator slots are kept wide, avoiding that the flux forced by the current closes in the stator iron without passing the air gap. Finite element calculations show that the computed torque of a machine model with wide open slots and a model having material parameters which have been changed to half closed slots differ with more than 3 % (table 1). The differences in the harmonics of the inductance are negligible (figure 4).

	slot opening	torque
Analytic calculated		16.30 Nm
FEM open slots	3.5 mm	15.31 Nm
FEM	2.3 mm	14.98 Nm
FEM half closed slots	1.6 mm	14.79 Nm

Tab. 1: Computed torque as a function of the slot opening

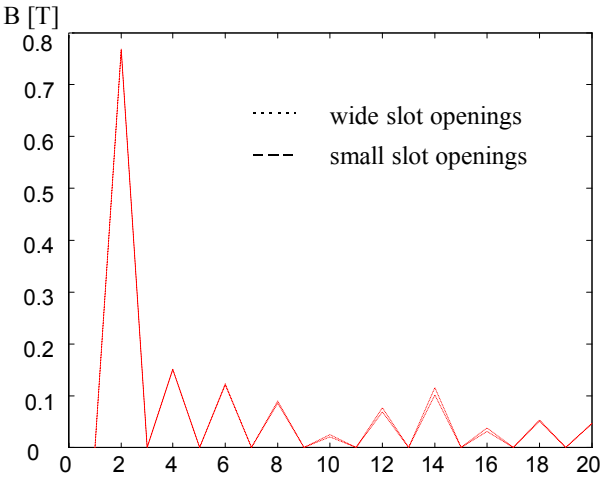

Fig. 4: Harmonics of the induction in the air gab as function of the slot opening

3.3 Rotor cage

Additional to the permanent magnets, the rotor has to carry a rotor cage in order to let the motor operate in "open loop" mode. Therefore, the angular magnet width is restricted to give way for the rotor bars. To maximise the influence of the rotor bars the air gap between the magnets, the q-axis, has to be larger than the opening of the rotor slots. Thus the motor has a significant saliency and can be compared to a machine with surface-inset magnets (figure 5). A benefit of the surface inset structure is that the torque giving force on the magnets is transferred to the rotor core by the iron between the magnets [4]. Furthermore the rotor surface can be smooth being rather important for the banding. A

disadvantage of this surface-inset type is an increased leakage of the magnetic flux. Also a higher torque ripple is caused by the saliency.

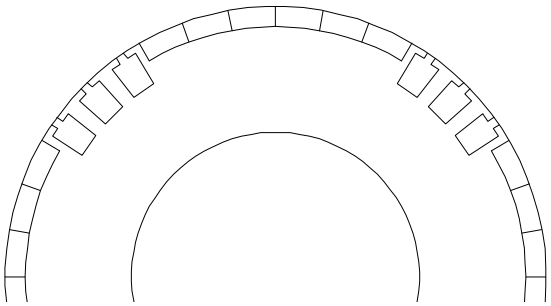

Fig. 5: Part of a cross sectional view of a 4-pole rotor

The rotor bars are narrowing the flux path and thus saturation of the q-axis may occur. These saturation effects can not be calculated analytically and are computed by the FEM. Figure 6a shows the plot of the flux lines of the magnetostatic solution of a permanent magnet machine at rated condition as calculated analytically without rotor bars. The computed torque is 6% lower than analytically calculated.

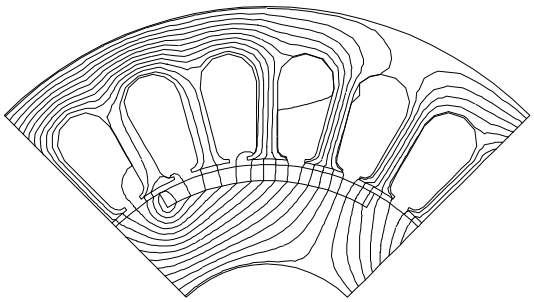

Fig. 6a: Flux lines for the PMSM without rotor bars

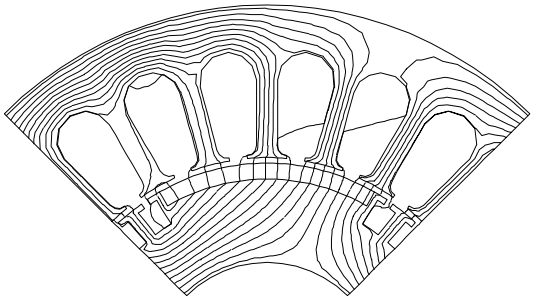

Fig. 6b: Flux lines for the PMSM with rotor bars between the permanent magnets

Figure 6b shows the flux plot for the same operating point, however with rotor bars which in synchronous mode magnetically are treated like air. The computed torque differs less than one percent from the calculation above, meaning that saturation due to the copper bars does not occur. The asymmetrical rotor cage has to ensure the start up of the V/f controlled motor and to balance disturbances. The start up is simulated by combining a PMSM as well as an induction machine. The dimensions of the rotor bars are calculated by computing the resistance and the current they have to carry requiring a cross section of about 20 mm^2.

In the start up procedure a slip is given, corresponding to the required start up current. The frequency has to fulfill the equation $f_2 = f_1 + p \cdot n$. If the machine has reached its synchronism f_2 is set to zero (figure 7).

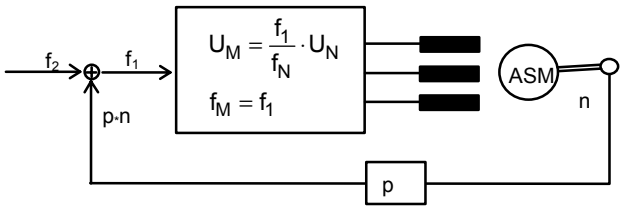

Fig. 7: Control scheme of the simulation of the start up procedure

Figure 8a shows the smooth start of the motor up to the demanded speed. The asynchronous torque becomes zero if the machine has reached the synchronism and the induced voltage tunes in on its stationary value (figure 8b).

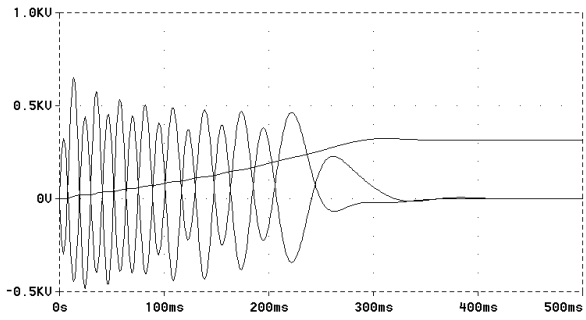

Fig. 8a: Asynchronous torque and the speed shown for the start up

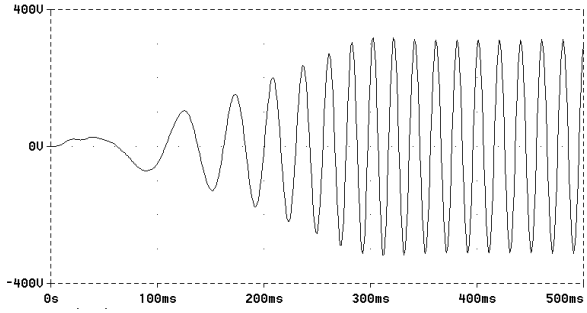

Fig. 8b: The induced voltage shown for the start up

3.4 Permanent magnet material

Another design aspect is the choice of the permanent magnet material. A high remanent flux density is needed, while a high coercivity is less important as overloads do not occur. NdFeB permanent magnets offer a high energy density as well as a high remanence flux density. Furthermore motors high temperatures are no more a drawback as the new generation of NdFeB magnets retains its magnetic properties up to temperatures of 130º C.

Using surface mounted magnet pieces, glued onto the rotor, instead of one magnet piece for one pole, reduces eddy current losses and the heating of the magnets.

3.5 Motor data

The design computation results in the following motor data:

Stack outer diameter	131 mm
Stack inner diameter	78.5 mm
Stack length	100 mm
Overall length	210 mm
Number of pole pairs	2
Slots per pole	2
Total mass	10.5 kg

Tab. 2a: Geometric motor data

Resistance	0.34 mΩ
Inductance in the q-axes	9.3 mH
Inductance in the d-axes	6.3 mH
Moment of inertia	0.0028 $kg*m^2$

Tab. 2b: Motor parameter

Rated speed	2200 rpm
Rated voltage	120 V
Rated current	16.0 A
Mechanical power (at 2200 rpm)	3710 W
Mechanical torque	16.3 Nm
efficiency	92.3 %

Tab. 2c: Motor parameters at steady state

4. MAGNETOSTATIC CALCULATION OF THE EQUIVALENT CIRCUIT

The high efficiency at partial load is shown by calculating the operating points of the equivalent circuit of the machine. As in irrigation system there are no dynamic requirements of the motor a static solution is sufficient.

U	n	I	T_m	P_m	η
$0.5*U_n$	1068	I_n	16.13	1.80	87.24
$0.6*U_n$	1300	I_n	16.11	2.19	89.06
$0.7*U_n$	1533	I_n	16.10	2.58	90.36
$0.8*U_n$	1765	I_n	16.09	2.97	91.31
$0.9*U_n$	1998	I_n	16.07	3.36	92.05
$1.0*U_n$	2230	I_n	16.06	3.75	92.62
$1.1*U_n$	2463	I_n	16.04	4.14	93.07

Tab. 3: Operating points of the equivalent circuit

5. MODIFIED INDUCTION MOTOR

In the framework of the development of this photovoltaic system, in the main part consisting of a 3.8 kW PMSM and a modified inverter matched to photovoltaic applications, the interactions between these components have to be examined. Therefore, a 3.2 kW standard induction motor is changed into a permanent magnet motor having a damper cage. The 5.5 kW solar inverter is designed for highly reliable operation even under severe conditions. The test installation is completed by a dc machine simulating the power provided by the solar cells and a centrifugal pomp.

Getting detailed information on the behaviour of a PMSM operating in “open loop” mode and supplied by a standard inverter for induction motors, is the main object of this part of the study. Experiences of this examination are taken into account in the motor development. Furthermore the higher efficiency of the permanent magnet motor at partial load can be demonstrated distinctly if the two compared motors have the same stator.

The 3.2 kW standard induction motor is modified by applying a new stator winding and a new rotor containing permanent magnets and an asymmetrical rotor cage. The rotor is under construction and measurements of the tests will be presented at the conference as well as the conclusion being drawn from this experiment.

6. CONCLUSIONS

In this paper the design of a PMSM for a photovoltaic irrigation system has been presented. The goal to get a high efficiency water pumping system has been reached by adapting the motor to the other components of the drive as well as by minimizing all kinds of losses. Rotor bars have been implemented in order start up the motor and to balance disturbances.

7. ACKNOWLEDGEMENTS

The authors are indebted to the Belgian Ministry of Scientific Research for granting the project IUAP No. 51

on Magnetic Fields. Furthermore, the research is supported by Flanders' Secretary of Economy.

8. REFERENCES

[1] Chang, L., Dawson, G. R., Eastham, T. R.: *Permanent Magnet Motor Design: Finite Elements and analytical Methods*. Proc. ICEM'90, Cambride (USA), pp. 1082-1088.

[2] Slemon, G. R.: Xian, L.: *Modelling and Design Optimisation of Permanent Magnet Motors. Electric Machines and Power Systems*, vol. 20, no. 2, April 1992, pp. 71-92.

[3] Nasar, S. A., Boldea, I., Unnewehr, L. E.: *Permanent Magnet, Reluctancs, and Self-Synchronous Motors*. CRC Press, 1993, London Tokyo

[4] Nipp, E.: *Alternative to Field Weakening of Surface Mounted Permanent Magnet Motors for Variable Speed Drives*. Proc. IAS'95, pp. 191-198.

[5] Sebastian T., Slemon, G. R., Rahman, M. A.: *Design Considerations for Variable Speed Permanent Magnet Motors*, Proc. ICEM'86, Munich, Sept. 1986, part 3, pp. 1099-1102.